Dalton Transactions

Accepted Manuscript

This article can be cited before page numbers have been issued, to do this please use: P. Ghosh, S. Bej, M. Nandi and T. K. Ghosh, *Dalton Trans.*, 2019, DOI: 10.1039/C9DT01067J.


This is an Accepted Manuscript, which has been through the Royal Society of Chemistry peer review process and has been accepted for publication.

Accepted Manuscripts are published online shortly after acceptance, before technical editing, formatting and proof reading. Using this free service, authors can make their results available to the community, in citable form, before we publish the edited article. We will replace this Accepted Manuscript with the edited and formatted Advance Article as soon as it is available.

You can find more information about Accepted Manuscripts in the author guidelines.

Please note that technical editing may introduce minor changes to the text and/or graphics, which may alter content. The journal's standard Terms & Conditions and the ethical guidelines, outlined in our author and reviewer resource centre, still apply. In no event shall the Royal Society of Chemistry be held responsible for any errors or omissions in this Accepted Manuscript or any consequences arising from the use of any information it contains.

ROYAL SOCIETY OF CHEMISTRY

rsc.li/dalton

View Article Online
DOI: 10.1039/C9DT01067J

Journal Name

ARTICLE

# Cu(II) templated formation of [n]Pseudorotaxanes (n= 2,3,4) using a tris-amino ether macrocyclic wheel and multidentate axles

Somnath Bej, Mandira Nandi, Tamal Kanti Ghosh and Pradyut Ghosh*

Received 00th January 20xx,
Accepted 00th January 20xx

DOI: 10.1039/x0xx00000x

www.rsc.org/

A tris-amine and oxy-ether functionalised macrocyclic wheel (**NaphMC**) and various phenanthroline based multidentate axles (**L1**, **L2** and **L3**) are utilised for the formation of [n]Pseudorotaxanes (n=2,3,4) in high yields *via* Cu(II) temptation and π–π stacking interactions. Systematic development of threaded supramolecular architectures *i.e.* [2]pseudorotaxane {**[2]CuPR(ClO$_4$)$_2$**}, [3]pseudorotaxane {**[3]CuPR(ClO$_4$)$_4$**} and [4]pseudorotaxane {**[4]CuPR(ClO$_4$)$_6$**} from bidentate **L1**, linear tetradentate **L2** and tripodal hexadentate **L3** respectively are described. All the [n]Pseudorotaxanes are well characterized by several spectroscopic and other experimental techniques such as electrospray ionization mass spectrometry (ESI-MS), Isothermal Titration Calorimetric (ITC) study, UV/Vis, EPR, IR and elemental analysis. Moreover, the single crystal X-ray analysis of [2]pseudorotaxane confirmed the threading of **L1** in the cavity of **NaphMC**, resulting in the formation of penta-coordinated Cu(II) ternary complex. ITC studies revealed the order of binding constant values for the formation of [n]Pseudorotaxanes from **NaphMC-Cu**(II) complex and multidentate axles as **L3** > **L2** > **L1**. Finally, we have also shown the ability of Ni(II) to act as a metal template in the formation of [n]Pseudorotaxanes.

## Introduction

In recent years, new generation of threaded molecular architectures such as pseudorotaxanes, rotaxanes and catenanes have shown immense interest to the scientific community for their synthetic challenges, structural complexities and other potential applications in various fields such as molecular machineries,[1] materials science,[2] polymer chemistry,[3] molecular sensor,[4] molecular recognition[4-5] and biological science.[6] Several threaded macromolecular architectures including mechanically interlocked molecules (MIMs) are synthesized by utilising various efficient non-covalent interactions such as cation/anion templation,[5b, 7] π-π stacking,[8] hydrogen bonding[9] and halogen bonding interactions.[10] Pseudorotaxanes are the essential building blocks for the synthesis of MIMs (*e.g.* rotaxanes, catenanes and knots) and prototypes for other molecular machineries which are of current interest in the field of supramolecular chemistry.[2b, 11] Development of synthetic threaded architectures having structural complexities is growing continuously and has led to the search for new wheels and axles for the construction of higher order [n]Pseudorotaxanes and relevant advanced architectures depending upon the binding strength of host-guest interactions.[7e, 12] In this regard, it is noteworthy to mention here that several research groups have explored the synthesis and other properties of [2]- and [3]pseudorotaxanes by utilising various approaches.[13] In this direction, numerous examples for the formation of [n]Pseudorotaxanes based on various type of wheels such as cryptand, pillar[n]arene, cucurbit[n]urils, cyclodextrin and crown ether *via* non-covalent interactions are widely reported.[14] However, synthesis and other applications of higher order metal ion templated threaded architechtures (e.g. [4]pseudorotaxane and higher) having interesting structural complexities are scarcely reported in literature.[11c, 15] In this regard, herein we report a systematic development of mono-, bi-, and tri-nuclear Cu(II) templated [2], [3], and [4]pseudorotaxanes respectively from **NaphMC** (Chart 1) and

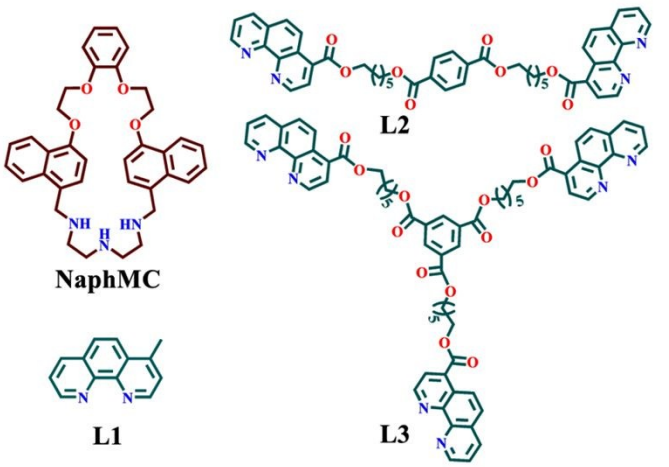


**Chart 1.** Chemical structure of macrocycle (**NaphMC**) and axles (**L1-L3**).

*School of Chemical Sciences, Indian Association for the Cultivation of Science, 2A & 2B Raja S. C. Mullick Road, Kolkata 700032, India. E-mail: icpg@iacs.res.in*

†Electronic Supplementary Information (ESI) available. CCDC 1892956. For ESI and crystallographic data in CIF or other electronic format See DOI: 10.1039/x0xx00000x

View Article Online DOI: 10.1039/C9DT01067J

newly synthesized tetra- and hexa-dentate axles (**L2** and **L3**) along with bi-dentate axle, **L1** (Chart 1). Involvement of metal ion coordination and π–π stacking interactions between the axles (**L1**-**L3**) and **NaphMC** resulted in significantly high yields of the [n]Pseudorotaxanes.

## Results and discussion

**Designing Aspects:**

Towards our goal of development of threaded architectures with structural diversities, we have strategically designed the macrocycle and multidentate axles to synthesize [n]Pseudorotaxanes with increasing structural complexities. Previously, our group reported tris amine based heteroditopic macrocycle and phenanthroline axle based selective formation of [2]pseudorotaxane with Cu(II) metal ion over other transition metal ions and bidentate axles.[13o, 14f] Moreover, we have also successfully demonstrated the efficient formation of [2]pseudorotaxanes in high yields from electron deficient bidentate 1,10-phenanthroline (**phen**) axle and electron rich naphthalene containing tris amine based macrocycle, **NaphMC** *via* Cu(II) temptation and π–π stacking interaction with high association constant values.[16] Inspired by the above mentioned results, herein we have utilized Cu(II) as a templating agent for the efficient synthesis of pseudorotaxanes. As we have also noticed that phenanthroline based axles showed high affinity towards the formation of pseudorotaxanes with Cu(II) and tris-amine based macrocycles, phenanthroline moiety has been incorporated in all the axles (**L1**-**L4**) as the metal binding unit. Accordingly, in order to synthesize higher homologues of [2]pseudorotaxane, we have introduced 4-methyl-1,10-phenanthroline (**L1**) as an axle (without affecting the coordination motif) to develop [2]pseudorotaxane {**[2]CuPR(ClO$_4$)$_2$**} where the substituted methyl group of **L1** can be further functionalized to produce multidentate axles for the preparation of higher order pseudorotaxanes. In this direction, we have synthesized bipodal-tetradentate axle, **L2** and tripodal-hexadentate axle, **L3** from **L1** for the synthesis of [3]pseudorotaxane {**[3]CuPR(ClO$_4$)$_2$**} and [4]pseudorotaxane {**[4]CuPR(ClO$_4$)$_2$**} having two and three chelating phenanthroline units respectively as shown in Fig. **1**. Chelating **phen** units are attached with a central benzene platform *via* aliphatic linkers in **L2** and **L3** in such a way that the pendant phenanthroline moieties are flexible enough to thread into multiple macrocycles (**NaphMC)** *via* coordination with Cu(II) to form higher order pseudorotaxanes. Interestingly, efficient binding of phenanthroline based axles with **NaphMC** and Cu(II) along with π–π stacking interactions between electron rich naphthyl unit of **NaphMC** and electron deficient **phen** unit of the axles can result in efficient synthesis of [n]Pseudorotaxanes (n=2,3,4) with high yields.

**Synthesis and Characterization of NaphMC, L2 and L3:**

The oxy-ether and tris-amine functionalised **NaphMC** was prepared by following the reported procedure[16] (Scheme 1S,

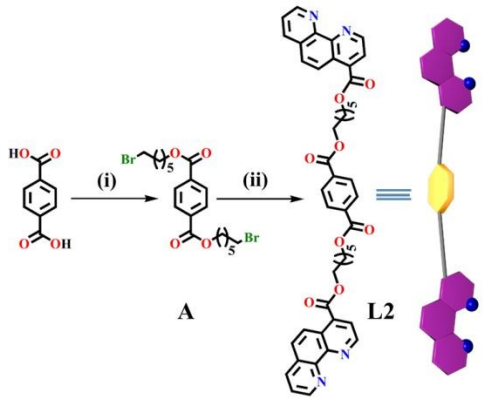


**Scheme 1.** Synthetic route of **L2**: (i) 1,6-dibromo hexane, $^t$BuOK, DMF, RT, 12h, reflux, another 18h, 68 %; (ii) Phen-Acid, TBAF, THF, RT, 12h, 74 %.

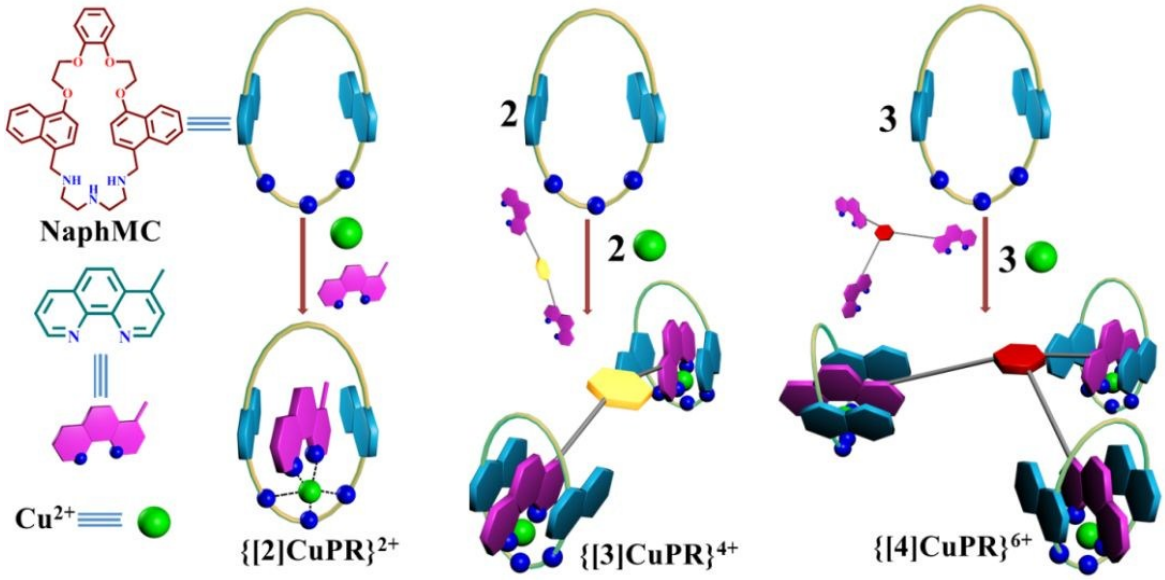


**Fig. 1** Cartoon- representation of designing strategies for the construction of transition metal based [n]Pseudorotaxane (n=2, 3, 4), Counter anions are omitted for clarity.

View Article Online
DOI: 10.1039/C9DT01067J

Journal Name

ARTICLE

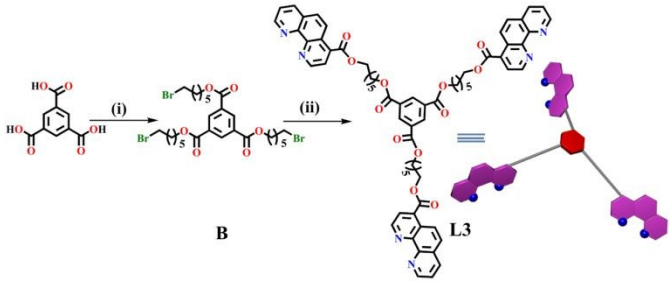


**Scheme 2.** Synthetic route of **L3**: (i) 1,6-dibromo hexane, $K_2CO_3$, DMF, RT, 24h, 83 %; (ii) Phen-Acid, TBAF, THF, RT, 12h, 78 %.

ESI†). 1, 10-phenanthroline-4-carboxylic acid (**Phen-Acid**) was also prepared from literature reported procedure[17] (Scheme 2S, ESI†) and further used for the synthesis of newly designed axles **L2** and **L3**. The synthetic route and chemical structures of **L2** and **L3** are shown in scheme **1** and **2** respectively. Both the axles **L2** and **L3** were synthesized in four steps with high yields as described in the experimental section. All of the above mentioned compounds were well characterized by $^1H$, $^{13}C$-NMR and mass spectrometric techniques as shown in ESI (Fig. 1S- Fig. 12S, ESI†).

### Synthesis and Characterization of [n]Pseudorotaxanes {[2]CuPR(ClO$_4$)$_2$, [3]CuPR(ClO$_4$)$_4$ and [4]CuPR(ClO$_4$)$_6$ }:

After the successful synthesis of **NaphMC**, **L2** and **L3**, we have carried out the synthesis of [n]Pseudorotaxanes (n=2,3,4) from **NaphMC**, $Cu(ClO_4)_2$ and corresponding axles (**L1**-**L3**). Initially, the macrocycle, **NaphMC** was reacted with $Cu(ClO_4)_2.6H_2O$ to form **NaphMC-Cu**(II) complex (Scheme 3S, ESI†) in $CHCl_3$-$CH_3OH$ (2:8) binary solvent mixture as reported previously.[16] After that, one equivalent of **L1** was added to the solution in situ at room temperature (RT). The resultant reaction mixture was stirred for 3-4h at RT and after that the solvent was evaporated to obtain **[2]CuPR(ClO$_4$)$_2$** as green solid in 83% yield (Scheme 3). By using similar reaction procedure as mentioned above, reaction of two equivalents of **NaphMC** and Cu(II) along with of one equivalent of tetra dentate ligand **L2** at RT led to the formation of [3]pseudorotaxanes {**[3]CuPR(ClO$_4$)$_4$**} in 79% yield (Scheme 3) and reaction of one equivalent of hexadentate tripodal **L3** along with three equivalent of **NaphMC** and Cu(II) in RT yielded [4]pseudorotaxanes {**[4]CuPR(ClO$_4$)$_6$**} in 71% yield (Scheme 3). Thorough synthetic procedures for the formation of [n]Pseudorotaxanes (n=2,3,4) are given in the experimental section. All the ternary complexes were well characterized by several spectroscopic and other experimental techniques (Fig. 13S- Fig. 41S, ESI†).

Detailed experimental studies were performed in order to

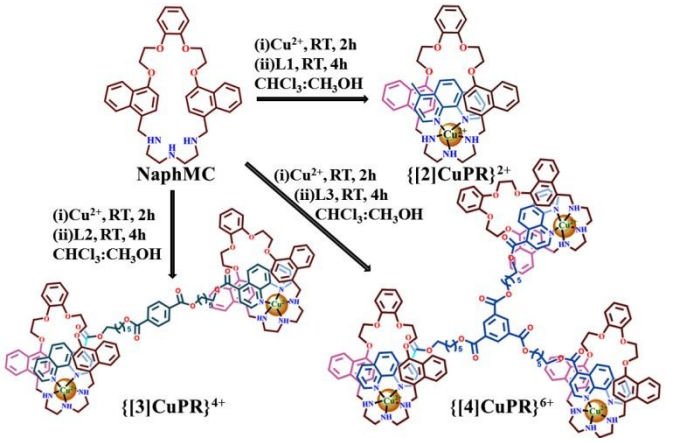


**Scheme 3**. Synthetic route of formation of [2], [3], [4]pseudorotaxanes **{([2]CuPR)$^{2+}$, ([3]CuPR)$^{4+}$ and ([4]CuPR)$^{6+}$}**. Counter anions are omitted for clarity.

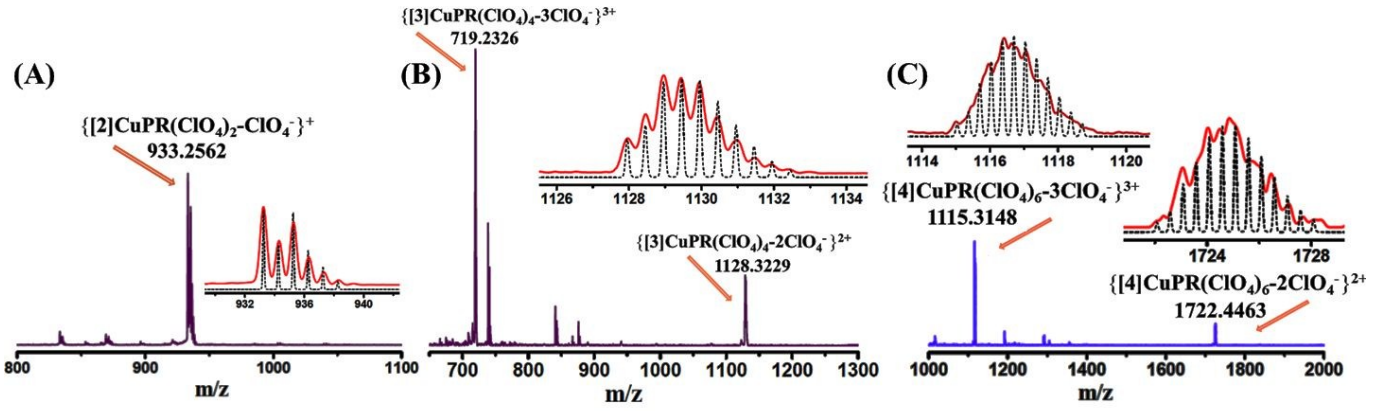


**Fig. 2:** ESI-MS (+ve) spectra of [2], [3], [4]pseudorotaxanes (A) **[2]CuPR(ClO$_4$)$_2$**, (B) **[3]CuPR(ClO$_4$)$_4$** and (C) **[4]CuPR(ClO$_4$)$_6$** with their isotopic distribution patterns of corresponding ion peak (inset shows red line for experimental and black line for calculated patterns of their isotopic distribution model).

View Article Online
DOI: 10.1039/C9DT01067J

# Journal Name

## ARTICLE





determine the formation of **[2]CuPR($ClO_4$)$_2$**, **[3]CuPR($ClO_4$)$_4$** and **[4]CuPR($ClO_4$)$_6$**. Initially, ESI-MS studies of **[2]CuPR($ClO_4$)$_2$** showed prominent molecular ion peaks at *m/z*= 933.2562 (calc. 933.2566) and 417.1539 (calc. 417.1541), which can be assigned to {**[2]CuPR($ClO_4$)$_2$-$ClO_4^-$**}$^+$ and {**[2]CuPR($ClO_4$)$_2$-2$ClO_4^-$**}$^{2+}$ species respectively (Fig. 2). Similarly, ESI-MS spectrum of **[3]CuPR($ClO_4$)$_4$** showed the presence of characteristic molecular ion peaks at *m/z* = 1128.3229 (calc. 1128.3223) and 719.2326 (calc. 719.2320), which correspond to the presence of {**[3]CuPR($ClO_4$)$_4$-2$ClO_4^-$**}$^{2+}$ and {**[3]CuPR($ClO_4$)$_4$-3$ClO_4^-$**}$^{3+}$ molecular species respectively (Fig 2). Finally, in case of **[4]CuPR($ClO_4$)$_6$**, prominent molecular ion peaks at *m/z*=1722.4463 (calc. 1722.4460) and 1115.3148 (calc. 1115.3144) indicated the presence of {**[4]CuPR($ClO_4$)$_6$-2$ClO_4^-$**}$^{2+}$ and {**[4]CuPR($ClO_4$)$_6$-3$ClO_4^-$**}$^{3+}$ respectively (Fig.13S- Fig.15S, ESI†). The isotopic distribution pattern of all the observed peaks matched well with the theoretical isotopic distribution pattern as obtained from the natural abundance of elements (Fig. 2). So, mass spectrometric analysis of all the pseudorotaxanes indicated their formation from **NaphMC** and respective axles.

**Isothermal Titration Calorimetric (ITC) Experiment:**

In order to get thermodynamic insight into the formation of [n]Pseudorotaxanes (n=2,3,4), ITC experiments were performed with **NaphMC**-**Cu**(II) and axles (**L1**-**L3**) in $CH_3CN$ at 298K. In all the ITC studies, respective axle solution in $CH_3CN$ is taken in the cell and titrated with **NaphMC**-**Cu**(II) solution in $CH_3CN$. Details of ITC experiments are provided in the experimental section and values of all the thermodynamic parameters (obtained from ITC titrations) are given in Table **1**. In all the cases, the titration data showed smooth and

Table 1: Thermodynamic parameter and association constants for **[2]CuPR($ClO_4$)$_2$**, **[3]CuPR($ClO_4$)$_4$** and **[4]CuPR($ClO_4$)$_6$** complex.

| Complex | Host | Guest | Fitting model | K ($M^{-1}$) | ΔH (Kcal/mol) | ΔS(cal/mol/deg) |
|---|---|---|---|---|---|---|
| **[2]CuPR($ClO_4$)$_2$** | **L1** | **NaphMC**-**Cu**(II) | One site | $K=1.06x10^6$ | $\Delta H$=-22.1 | $\Delta S$=-46.5 |
| **[3]CuPR($ClO_4$)$_4$** | **L2** | **NaphMC**-**Cu**(II) | Sequential two sites | $K_1=1.04x10^5$<br>$K_2=3.14x10^4$ | $\Delta H_1$=-58.4<br>$\Delta H_2$=-167.1 | $\Delta S_1$=-173.0<br>$\Delta S_2$=-539.0 |
| **[4]CuPR($ClO_4$)$_6$** | **L3** | **NaphMC**-**Cu**(II) | Sequential three sites | $K_1=1.34x10^6$<br>$K_2=6.27x10^4$<br>$K_3=1.34x10^5$ | $\Delta H_1$=-8.2<br>$\Delta H_2$=-11.4<br>$\Delta H_3$=-2.9 | $\Delta S_1$=0.464<br>$\Delta S_2$=-16.1<br>$\Delta S_3$=13.8 |

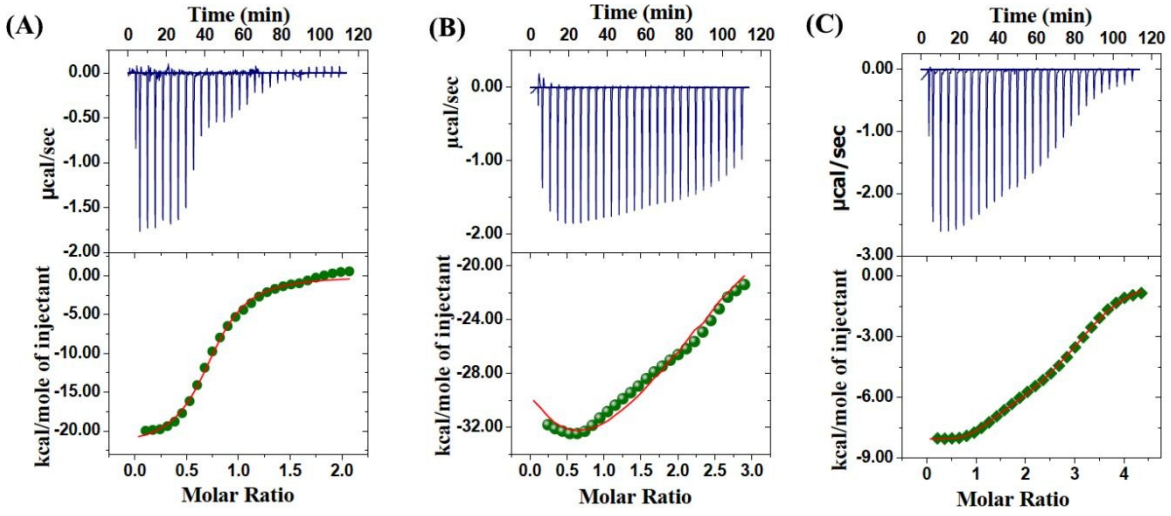


**Fig. 3:** Isothermal titration calorimetric titration plots (A) between **L1** (0.02 mM) and **NaphMC**-**Cu**(II) solution (0.2 mM); (B) between **L2** (0.01 mM) and **NaphMC**-**Cu**(II) solution (0.14 mM);(C) between **L3** (0.04 mM) and **NaphMC**-**Cu**(II) solution (0.84 mM) at 298 K in $CH_3CN$. In all the graphs, upper part shows the heat flow experimentally observed in each titration against time. The lower part signifies integrated isotherms(acquired by integrating the peaks of the above plot) vs molar ratio (A) one site binding model and (B, C) sequential binding model (n = 2,3 respectively).

View Article Online
DOI: 10.1039/C9DT01067J

Journal Name

ARTICLE



exothermic titration profiles which were fitted to the appropriate binding models. In case of titration of **NaphMC-Cu**(II) with **L1**, the titration data points were fitted to one site binding model which showed exothermic binding process with binding constant value of $1.06x10^6$ (Fig. 3, Table 1). On the other hand, during the titration of **NaphMC-Cu**(II) with **L2**, titration data points were fitted to a sequential two sites binding model which yielded the binding constant values of $K_1$ = $1.04x10^5$ and $K_2$ = $3.14x10^4$ (Fig. 3, Table 1). Finally, titration of **NaphMC-Cu**(II) with **L3** gave the binding constant values of $K_1$ = $1.34x10^6$, $K_2$ = $6.27x10^4$ and $K_3$=$1.34x10^5$ upon fitting the titration data points to sequential three sites binding model (Fig. 3, Table 1). It is clearly evident from table 1 that binding processes of **NaphMC-Cu**(II) with **L1**-**L3** were highly enthalpy and entropy driven processes which led to high binding constant values in case of all the pseudorotaxanes with the following order **L3** > **L2** > **L1**.

**Photophysical Studies:**

In order to revalidate the experimental results obtained from ITC studies for the binding of **L1**-**L3** with **NaphMC-Cu**(II), UV/Vis titration experiments were carried out between axles (**L1**-**L3**) and **NaphMC-Cu**(II) in $CH_3CN$ at 298K. UV/Vis titration between **NaphMC-Cu**(II) and **L1** suggested that the absorption maxima of **L1** at 263 nm (n-$\pi$* transition) decreases with concomitant increase of new absorption maxima at 277 nm (Fig. 4), which matched well with the general pattern of change in absorption maxima with similar kind of threaded [2]pseudorotaxanes having analogous tris-amine macrocycle, phenanthroline based axle and Cu(II) salt.[13m, 16] In case of titration of **L2** and **L3** with **NaphMC-Cu**(II), absorption maxima of **L2** and **L3** at 274 nm and 275 nm respectively decreases gradually with concomitant generation of new absorption maxima at 281 nm and 282 nm respectively (Fig. 4). Thus, the change in absorption characteristics during the formation of **[3]CuPR(ClO$_4$)$_4$** and **[4]CuPR(ClO$_4$)$_6$** are similar with that of **[2]CuPR(ClO$_4$)$_2$** (Fig. 4). As the metal center and the binding units of axle and macrocycles are similar in cases of [2], [3] and [4]pseudorotaxanes, correlating similar changes in absorption characteristics during the formation of all the pseudorotaxanes supported the threading of **L2** and **L3** inside the macrocycle during the formation of [3] and [4]pseudorotaxanes respectively. These process got saturated after addition of nearly one, two and three equivalents of **NaphMC-Cu**(II) into the solution of **L1**, **L2** and **L3** respectively (Fig. 16S- Fig. 18S, ESI†). Molar ratio plot analysis for the above three titrations showed the existence of 1: 1, 1: 2 and 1: 3 {axle: **NaphMC-Cu**(II)} complex in solution for **L1**, **L2** and **L3** respectively (Fig. 19S- Fig. 21S, ESI†). Furthermore, the isolated threaded complexes showed characteristic absorption maxima ($\lambda_{max}$) at 276 nm, 282 nm and 283 nm for [2], [3] and [4]pseudorotaxanes respectively (Fig. 22S(A), ESI†). Interestingly, the absorption maxima of all the isolated complexes of **{[2]CuPR(ClO$_4$)$_2$}**, **{[3]CuPR(ClO$_4$)$_4$}** and **{[4]CuPR(ClO$_4$)$_6$}** obtained by reacting **NaphMC-Cu**(II) with **L1**, **L2**, and **L3** respectively, matched perfectly with the final spectra of respective UV/Vis titration experiments (Fig. 4) which indicated the formation of the corresponding pseudorotaxanes. Absorption titration data points for the titration of **NaphMC-Cu**(II) with **L1** were fitted to a one site binding model *via* non-linear fitting model which yielded binding constant value of $3.08x10^6$ $M^{-1}$ (Fig. 23S, ESI†). Similarly, fitting of titration data points of **NaphMC-Cu**(II) with **L2** yielded binding constant values of $1.48x10^6$ $M^{-1}$ and $3.77x10^5$ $M^{-1}$ for $K_1$ and $K_2$ respectively (Fig. 24S, ESI†). As appropriate binding model for fitting the data points of 1:3 (H:

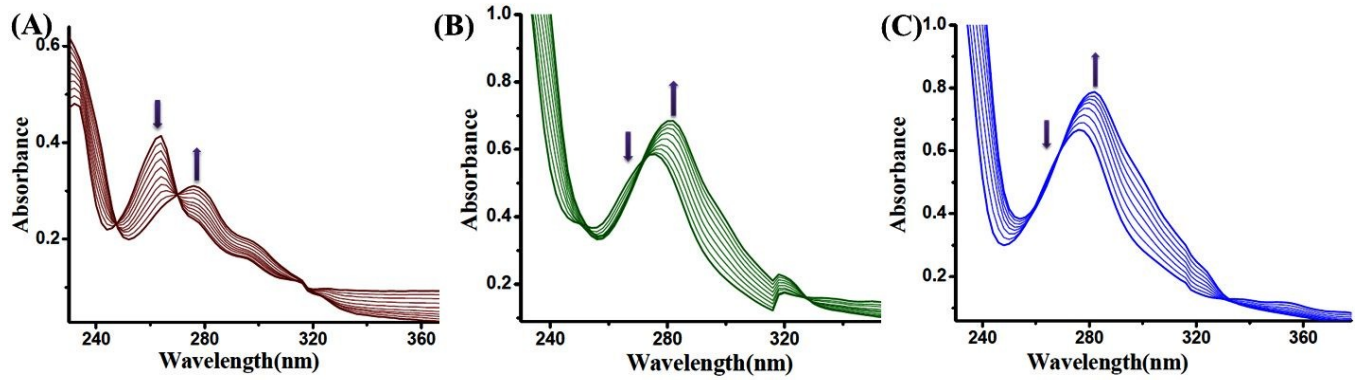


**Fig. 4.** UV/Vis titration profile:(A) between **L1** ($1x10^{-5}$ M) with **NaphMC-Cu**(II) ($1x10^{-4}$ M) in $CH_3CN$ at 298 K, (B) between **L2** ($1x10^{-5}$ M) with **NaphMC-Cu**(II) ($2.8x10^{-4}$ M) in $CH_3CN$ at 298 K, (C) between **L3** ($1x10^{-5}$ M) with **NaphMC-Cu**(II) ($4.4x10^{-4}$ M) in $CH_3CN$ at 298 K.

View Article Online
DOI: 10.1039/C9DT01067J

Journal Name

ARTICLE



G) stoichiometric binding was not available, we could not determine the binding constant values for the formation of **[4]CuPR(ClO$_4$)$_6$** from **NaphMC**-**Cu**(II) and **L3**. As we moved from [2]pseudorotaxane to [3] and [4]pseudorotaxanes, we did not observe any significant alteration in the properties of the threaded complexes. However, on-going from [2]pseudorotaxane to [3] and [4]pseudorotaxanes, minor shift of the absorption maxima corresponding to n-π* transition from 276 nm to 282 nm and 283 nm were observed respectively. All the pseudorotaxanes were found to be non-emissive in nature when they were excited at their respective absorption maxima (Fig. 22S(B), ESI†).

**Single Crystal X-Ray Diffraction Analysis:**

In order to determine the coordination environment around Cu(II) in the pseudorotaxanes by single crystal X-ray spectroscopy, considerable amount of efforts were given to crystallize all the pseudorotaxanes. Single crystals of [2]pseudorotaxane, **[2]CuPR(OTf)$_2$** were obtained by exchanging **ClO$_4^-$** counter anion of **[2]CuPR(ClO$_4$)$_2$** with **OTf$^-$** anion. Green colored single crystals of **[2]CuPR(OTf)$_2$** were obtained upon slow evaporation of a solution of **[2]CuPR(ClO$_4$)$_2$** and excess NaOTf in $CH_3CN$ (Fig. 5). All the crystallographic details are provided in ESI† (Table 1S and Fig. 25S- Fig. 27S). Detailed crystal structure analysis showed that, **OTf$^-$** based [2]Pseuorotaxane adopts penta-coordinated arrangement around the central Cu(II) centre, in which three coordination sites are provided by tris amine of **NaphMC** and remaining two coordination sites are occupied by the bidentate phenanthroline unit of **L1**. Structural parameter (τ) value of 0.638 which is in between the geometrical spectrum of square pyramidal and trigonal bipyramidal geometries, suggested the presence of distorted TBP geometry in **[2]CuPR(OTf)$_2$**. Significantly short distance of 3.372 and 3.405 Å between the electron rich naphthyl unit of **NaphMC** and electron deficient phenanthroline unit of **L1** in the complex suggested the existence of π–π stacking interactions in solid state. Ellipsoid and space-filling model in Fig. 5 revealed complete threading of **L1** inside the cavity of **NaphMC** in [2]pseudorotaxane. However, even after several attempts, we could not isolate single crystals of [3]- and [4]pseudorotaxanes. As a result, the exact coordination environment around Cu(II) centres in these two complexes could not be determined.

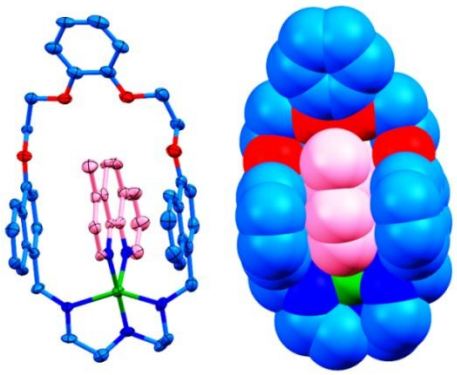

**Fig. 5:** Ellipsoid model (40% probability level) and space-filling model of **([2]CuPR)$^{2+}$.** Counter anions and hydrogens are omitted for clarity.

**EPR Characterization:**

In order to determine the coordination geometry of Cu(II) in all the synthesized mono-, bi- and tri-nuclear Cu(II) templated pseudorotaxanes, all of them were subjected to X-band EPR spectroscopy at 80K in $CH_3CN$. The values of g parameters and EPR spectra of **[2]CuPR(ClO$_4$)$_2$**, **[3]CuPR(ClO$_4$)$_4$** and **[4]CuPR(ClO$_4$)$_6$** in $CH_3CN$ are provided in Table 2 and ESI† (Fig. 28S- Fig. 30S, ESI†). In all the cases, EPR spectra showed the pattern of $g_{||} > g_{\perp}$ (Table 2) which indicated the presence of the unpaired electron in $d_{x^2-y^2}$ orbital of **Cu**(II) in all the complexes. This result clearly indicated that **Cu**(II) centre is present in a distorted square pyramidal geometrical arrangement upon coordination of axle with the **NaphMC**-**Cu**(II) in all the ternary complexes as reported previously.[14f, 14g]

Now, it should be mentioned here that the flexibility of the phenanthroline binding unit in bi and tripodal axles (**L2** and **L3**) through the attachment of aliphatic spacer between central benzene ring and pendant phenanthroline units are critical criteria for the formation of higher order [3] and [4]pseudorotaxanes. In this regard, we have synthesized a new ester functionalised tripodal hexadentate axle, **L4** which contains less flexible C2-alkyl chain spacer unit instead of more flexible C6-alkyl chain spacer (**L3**) attached with benzene platform. **L4** was synthesized in four steps via tribromo ester, **C** in 68.8% yield (Scheme 4S and Fig. 31S- Fig. 35S, ESI†). After successful synthesis of **L4**, we have examined it's ability towards the formation of Cu(II) templated [4]pseudorotaxanes

**Table 2.** $g_{||}$, $g_{\perp}$ values for the [n]Pseudorotaxanes (n=2,3,4)

| Complex | $g_{||}$ | $g_{\perp}$ |
|---|---|---|
| **[2]CuPR(ClO$_4$)$_2$** | 2.22806 | 2.02293 |
| **[3]CuPR(ClO$_4$)$_4$** | 2.22132 | 2.01676 |
| **[4]CuPR(ClO$_4$)$_6$** | 2.24085 | 2.02176 |

by ESI-MS and UV/Vis spectroscopic studies. ESI-MS analysis showed molecular ion peak at m/z=1699.4115 (calc. 1699.4113), corresponding to [**NaphMC.Cu**(II)**.L4.ClO$_4^-$**]$^+$, which indicated the formation of [2]pseudorotaxane only without the presence of any peaks corresponding to other higher order pseudorotaxanes (Fig. 36S, ESI†). On the other hand, the UV/Vis titration experiment between **NaphMC-Cu**(II) and **L4** showed gradual decrease in intensity of the parent absorption band at $\lambda_{max}$= 276 nm with simultaneous generation of a new peak at $\lambda_{max}$= 280 nm upon addition of **NaphMC-Cu**(II) in the axle (**L4)** solution in $CH_3CN$ (Fig. 37S, ESI†). Analysis of titration data showed the formation of 1:1 {**NaphMC-Cu**(II): **L4**} complex in solution (Fig. 38S, ESI†) which indicated the formation of only [2]pseudorotaxane among other higher order pseudorotaxanes. Thus, less flexible C2-alkyl spacer based axle, **L4** failed to produce higher order [3] and [4]pseudorotaxanes as opposed to more flexible C6-alkyl spacer based axle, **L3**.

Furthermore, in order to investigate the efficiency of other transition metal {except Cu(II)} in the synthesis of [n]Pseudorotaxanes (n=2,3,4), $Ni(ClO_4)_2{\cdot}6H_2O$ was employed as another transition metal templating agent for the synthesis of [n]Pseudorotaxanes (n=2,3,4). In this direction, we have synthesized **NaphMC-Ni**(II) complex (Scheme 5S, ESI†) and pseudorotaxanes (Scheme 6S, ESI†) by following the similar procedure of formation of Cu(II) templated [n]Pseudorotaxanes (n=2,3,4) as mentioned in the experimental section. Formation of **NaphMC-Ni**(II) complex was supported by ESI-MS analysis which showed the presence of a prominent molecular ion peak at m/z=734.1778 (calc. 734.1779), that revealed the presence of {**NaphMC.Ni**(II)**.ClO$_4^-$**}$^+$ species (Fig. 42S, ESI†). Afterwards, Ni(II) templated [n]pseudorotaxanes (n=2,3,4) were prepared and characterized by ESI-MS, UV/Vis and elemental analysis studies. ESI-MS of **[2]NiPR(ClO$_4$)$_2$**, **[3]NiPR(ClO$_4$)$_4$** and **[4]NiPR(ClO$_4$)$_6$** complexes showed the presence of the molecular ion peaks at m/z = 928.2621 (calc. 928.2623), 2345.6048 (calc. 2345.6046) and 1714.9547 (calc. 1714.9546) which correspond to **{[2]NiPR(ClO$_4$)$_2$-ClO$_4^-$}$^+$**, **{[3]NiPR(ClO$_4$)$_4$-ClO$_4^-$}$^+$** and **{[4]NiPR(ClO$_4$)$_6$-2ClO$_4^-$}$^{2+}$** species respectively (Fig. 43S- Fig. 45S, ESI†). The experimentally observed isotopic distribution patterns of all the complexes matched well with the simulated patterns which are obtained from natural abundance of the elements. Additionally, UV/Vis titration studies were performed towards the formation of Ni(II) templated pseudorotaxanes with **NaphMC-Ni**(II) complex and all the axles (**L1**-**L3**). The absorption maxima of the **L1**, **L2** and **L3** at 263 nm, 274 nm and 275 nm gradually decreases with concomitant increase in absorption maxima at 274 nm, 283 nm and 284 nm respectively upon addition of **NaphMC-Ni**(II) complex in the axle solutions (Fig. 46S- Fig. 48S, ESI†). Molar ratio plot analysis from all the above mentioned titrations indicated the formation of 1: 1, 1: 2 and 1: 3 {axle: **NaphMC-Ni**(II)} complexes in cases of **[2]NiPR(ClO$_4$)$_2$**, **[3]NiPR(ClO$_4$)$_4$** and **[4]NiPR(ClO$_4$)$_6$** respectively (Fig. 49S- Fig. 51S, ESI†). Additionally, absorption maxima of all the isolated complexes of **[2]NiPR(ClO$_4$)$_2$**, **[3]NiPR(ClO$_4$)$_4$** and **[4]NiPR(ClO$_4$)$_6$** obtained by reacting **NaphMC-Ni**(II) with **L1, L2,** and **L3** respectively (Fig. 52S, ESI†), matched perfectly with the final spectra of UV/Vis titration experiments (Fig. 46S- Fig. 48S, ESI†) which indicated the formation of respective pseudorotaxanes.

## Conclusions

In summary, we have demonstrated the systematic development of [2]-, [3]-, and [4]pseudorotaxanes from bidentate, bipodal-tetradentate and tripodal- hexadentate axles respectively *via* Cu(II) temptation and π–π stacking interactions using an amino ether macrocyclic wheel. Further, efficiency of Ni(II) as a metal template for the formation of [2]-, [3]-, and [4]pseudorotaxanes has also been demonstrated. We are currently focusing on the construction of higher generation pseudorotaxanes and rotaxanes consist of various functional groups towards the development of new materials.

## Experimental Section

### General details

All reactions were carried out under the atmosphere of argon gas. Commercially available reagents were purchased and used as received. Solvents were dried following the literature procedures. Copper perchlorate was stored in a vacuum desiccator and used for experiments. The electronic spray ionization (ESI) mass spectra were carried out by using solvent ($CH_3CN$/ $CH_3OH$) on a QToF–Micro YA 263 Mass spectrometer in positive ion mode. $^1$H NMR and $^{13}$C NMR spectra were recorded on an FT-NMR Bruker DPX 400/500 MHz NMR spectrometer. The absorption studies were carried out using Perkin-Elmer Lambda 900 UV–Vis–NIR spectrometer with quartz cuvette of 1 cm path length. The isothermal titration calorimetric (ITC) studies were carried out with a Micro-Cal VP-ITC instrument using HPLC grade $CH_3CN$ at 298K. Elemental analysis was performed by using Perkin-Elmer 2500 series II elemental analyzer, Perkin-Elmer, USA. EPR spectra were recorded by using a JEOL JES-FA200 spectrometer with an X band micro web unit. Fourier transform infrared (FT-IR) studies were performed on a SHIMADZU FTIR-8400S IR spectrophotometer with KBr pellets.

### Synthesis of NaphMC and Phen-Acid:

Naphthalene containing oxy-ether and tris-amine functionalized macrocycle (**NaphMC**) was prepared *via* three step process by following the reported procedure.[16] 1,10-phenanthroline-4-carboxylic acid (**Phen-Acid**) was also synthesized by using literature procedure.[17] The characteristic data of **NaphMC** and **Phen-Acid** were perfectly matched with the reported data.

### Synthesis of compound A:

Terephthalic acid (332 mg, 2 mmol) and excess 1,6-di bromohexane (1216 μL, 8 mmol) were reacted in DMF medium in presence of potassium *tert*-butoxide (561 mg, 5 mmol) at room temperature (RT) under argon atmosphere for 12h then the reaction mixture was refluxed for another 18h. The reaction was cooled to RT and evaporated to dryness under vacuum. The crude was dissolved in excess of $CHCl_3$ and

View Article Online
DOI: 10.1039/C9DT01067J



filtered by using sintered crucible. After complete evaporation of the filtrate, the crude residue was purified *via* silica gel column chromatography using 3% ethylacetate-hexane as eluent and the oily liquid product was obtained as compound **A**, which was characterized as pure form. Yield 403 mg (68%). HRMS (ESI-MS): *m/z* calculated for $C_{20}H_{28}Br_2NaO_4$ [Comp **A** +Na]$^+$ = 513.0252, found = 513.0278. $^1$H NMR (400 MHz, $CDCl_3$): δ (ppm) 1.48-1.53 (m, 8H, -$CH_2$), 1.79-1.91 (m, 8H, -$CH_2$), 3.42 (t, 4H, J = 6.4 Hz ,- $CH_2$), 4.35 (t, 4H, J = 6.8 Hz ,-$OCH_2$), 8.10 (s, 4H, Ar-H). $^{13}$C NMR (100 MHz, $CDCl_3$): δ (ppm) 25.4, 28.0, 28.7,32.8, 33.8, 65.4, 129.7, 134.3, 166.0.

**Synthesis of axle L2:**

**Phen-Acid** (67 mg, 0.3 mmol) was dissolved in dry THF in presence of tetra-n-butyl ammonium fluoride (TBAF) (95 mg, 0.3 mmol). Compound A (49 mg, 0.1 mmol) was added dropwise at 0°C to the reaction mixture. The reaction mixture was stirred at RT for 12h under argon atmosphere. After that the solvent was removed under vacuum and the product was extracted with $CHCl_3$ and water, by washing the organic layer repeatedly with $NaHCO_3$ and brine solution. Then, the organic layer was evaporated and dried completely in *vacuo* after dried over anhydrous sodium sulfate. The solid was isolated and characterized as pure form. Yield 11.7 mg (74%). HRMS (ESI-MS): m/z calculated for $C_{46}H_{42}N_4NaO_8$ [**L2** +Na]$^+$ = 801.2900, found = 801.2907. $^1$H NMR (500 MHz, $CDCl_3$): δ (ppm) 1.58 (br, 8H, -$CH_2$), 1.83-1.92 (m, 8H, -$CH_2$), 4.37 (t, 4H, J = 6.5 Hz, - $OCH_2$), 4.50 (t, 4H, J = 7.0 Hz, - $OCH_2$), 7.68 (q, 2H, J = 4.0 Hz, Ar-H), 7.91 (d, 2H, J = 9.0 Hz, Ar-H), 8.09 (m, 6H, Ar-H), 8.28 (d, 2H, Ar-H), 8.79 (d, 2H, J = 9.0 Hz, Ar-H), 9.22 (d, 2H, J = 3.0 Hz, Ar-H), 9.29 (d, 2H, J = 4.5 Hz, Ar-H). $^{13}$C NMR (100 MHz, $CDCl_3$): δ (ppm) 25.9, 25.9, 28.8, 65.4, 66.1, 123.6, 123.7, 123.8, 126.2, 128.2, 128.5, 129.7, 134.3, 135.5, 136.0, 149.8, 150.8, 165.9, 166.4.

**Synthesis of compound B:**

Excess of 1,6-di bromohexane (912 µL, 6 mmol) was added to the mixture of benzene-1,3,5-tricarboxylic acid (210 mg, 1 mmol), and anhydrous $K_2CO_3$ (828 mg, 6 mmol) in DMF at RT under argon gas for 24h. The DMF was evaporated under vacuum and the reaction mixture was extracted with $CHCl_3$ and water. The organic layer was washed repeatedly by brine solution and dried over anhydrous sodium sulfate. The organic solvent was evaporated in *vacuo* and to removed excess 1,6-dibromohexane from the crude, filtering column chromatography was performed by using 60-120 mesh silica gel with 4% ethylacetate-hexane as eluent. The product compound **B** was isolated as liquid form of and characterized. Yield 276.4 mg (83%). HRMS (ESI-MS): m/z calculated for $C_{27}H_{40}Br_3O_6$ [Comp **B** +H]$^+$ = 697.0375, found = 697.0371. $^1$H NMR (400 MHz, $CDCl_3$): δ (ppm) 1.49-1.54 (m, 12H, -$CH_2$), 1.79-1.94 (m, 12H, -$CH_2$), 3.42 (t, 6H, J = 6.8 Hz, -$CH_2$), 4.39 (t, 6H, J = 6.8 Hz, -$OCH_2$), 8.83 (s, 3H, Ar-H). $^{13}$C NMR (100 MHz, $CDCl_3$): δ (ppm) 25.4, 28.0, 28.7, 32.8, 33.7, 65.7, 131.6, 134.6, 165.2.

**Synthesis of axle L3:**

TBAF (142 mg, 0.45 mmol) was added to dissolve the Phen-Acid (100 mg, 0.45 mmol) in dry THF and Compound **B** (70 mg, 0.1 mmol) was added dropwise to the reaction mixture at 0°C at stirring condition. The reaction mixture was allowed to stir at RT for 12h maintaining the inert atmosphere. Then, the solvent was evaporated under vacuum and was extracted with $CHCl_3$ and water by washing the organic layer with $NaHCO_3$ and brine solution (three times). The organic layer were collected and dried over anhydrous sodium sulfate. After the evaporation desired compound was isolated and characterized as solid axle **L3**. Yield 12.6 mg (78%). HRMS (ESI-MS): m/z calculated for $C_{66}H_{61}N_6O_{12}$ [**L3** +H]$^+$ = 1129.4347, found = 1129.4349. $^1$H NMR (400 MHz, $CDCl_3$): δ (ppm) 1.73-1.89 (m, 24H, -$CH_2$), 4.37-4.50 (m, 12H, -$CH_2$), 7.65-7.68 (m, 3H, Ar-H), 7.89 (d, 3H, J = 9.2 Hz, Ar-H), 8.09 (d, 3H, J = 4.4 Hz, Ar-H), 8.26 (d, 3H, J = 7.6 Hz, Ar-H), 8.76-8.82 (m, 6H, Ar-H), 9.20-9.29 (m, 6H, Ar-H). $^{13}$C NMR (100 MHz, $CDCl_3$): δ (ppm) 25.9, 25.9, 28.7, 65.8, 66.1, 123.6, 123.7, 123.8, 126.2, 128.2, 128.5, 131.6, 134.6, 135.5, 136.0, 146.1, 147.4, 149.9, 150.8, 165.2, 166.4.

**Synthesis of compound C:**

Compound **C** was synthesized by following the similar synthetic procedure as compound **B**. Compound **C** was isolated as solid form and was characterized thoroughly. Yield: 86%. $^1$H NMR (400 MHz, $CDCl_3$): δ (ppm) 3.68 (t, 6H, J = 6.0 Hz, -$CH_2$), 4.70 (t, 6H, J = 6.0 Hz, -$CH_2$), 8.91 (s, 3H, Ar-H). $^{13}$C NMR (100 MHz, $CDCl_3$): δ (ppm) 28.4, 65.0, 131.1, 135.3, 164.4.

**Synthesis of axle L4:**

Axle **L4** was prepared by following a similar procedure as axle **L3**. The product was isolated and characterized. Yield: 80%. HRMS (ESI-MS): m/z calculated for $C_{54}H_{37}N_6O_{12}$ [**L4** +H]$^+$ = 961.2469, found = 961.2468. $^1$H NMR (500 MHz, $CDCl_3$): δ (ppm) 4.67-4.83 (m, 12H, -$CH_2$), 7.64-7.69 (m, 3H, Ar-H), 7.80-7.85 (m, 3H, Ar-H), 8.07-8.11 (m, 3H, Ar-H), 8.23-8.29 (m, 3H, Ar-H), 8.67-8.72 (m, 3H, Ar-H), 8.90-8.99 (m, 3H, Ar-H), 9.20-9.30 (m, 6H, Ar-H). $^{13}$C NMR (125 MHz, $CDCl_3$): δ (ppm) 63.4, 63.5, 123.7, 123.8, 123.9, 126.1, 128.3, 128.4, 131.3, 134.6, 135.2, 135.6, 136.3, 147.0, 149.9, 150.6, 164.6, 165.9.

**Synthesis of [2]pseudorotaxanes {[2]CuPR($ClO_4$)$_2$}:**

**NaphMC** (58 mg, 0.1 mmol) was dissolved in $CHCl_3$ and $Cu(ClO_4)_2$ .$6H_2O$ (37 mg, 0.1 mmol) in $CH_3OH$ was added to it. The reaction mixture was stirred for 2h at RT. In situ, equivalent amount of bidentate chelating ligand (**L1)** (19.4 mg, 0.1 mmol) was added to the above reaction mixture. The resultant mixture was stirred at RT for another 3-4h. As a result, Cu(II) templated heteroleptic ternary complex *i.e.* [2]pseudorotaxane **{[2]CuPR($ClO_4$)$_2$}** was formed. Then, the solvent was evaporated and dried. By washing the solid residue with $CHCl_3$ and diethylether, the greenish colored solid was isolated as **{[2]CuPR($ClO_4$)$_2$}** in yield 83%. Anal. calcd. For **[2]CuPR($ClO_4$)$_2$**, $C_{49}H_{49}Cl_2CuN_5O_{12}$ (MW = 1034.39) C, 56.90; H, 4.77; N, 6.77; found: C, 56.23; H, 4.71; N, 6.48. HRMS (ESI-MS) {**[2]CuPR($ClO_4$)$_2$-$ClO_4^-$**} =$C_{49}H_{49}ClCuN_5O_8$}$^+$: calcd, *m/z* =

933.2566; found, *m/z* = 933.2562; {**[2]CuPR(ClO$_4$)$_2$-2ClO$_4^-$** =$C_{49}H_{49}CuN_5O_4$}$^{2+}$: calcd, *m/z* = 417.1541; found, *m/z* = 417.1537; IR (KBr, ν cm$^{-1}$): 437, 462, 518, 671, 765, 821, 848, 933, 1089, 1120, 1143, 1232, 1251, 1278, 1396,1431, 1456, 1506, 1581, 1649, 2921, 3421. Absorption spectra studies: $\lambda_{max}$= 276 nm in $CH_3CN$ solvent and molar extinction coefficient value in $CH_3CN$ (ε) = 3.14x10$^4$ M$^{-1}$ cm$^{-1}$.

**Synthesis of [3]pseudorotaxane {[3]CuPR(ClO$_4$)$_4$}:**

$Cu(ClO_4)_2.6H_2O$ (37 mg, 0.1 mmol) was dissolved in $CH_3OH$ and added to a solution of **NaphMC** (58 mg, 0.1 mmol) in $CHCl_3$. The reaction mixture was stirred at RT for 2h. Then, the tetradentate chelating ligand (**L2**) (38 mg, 0.05 mmol) was added to the above reaction mixture. The resultant mixture was stirred for another 3-4h at RT. Afterward, solvent was removed by vacuum and the crude product was washed with $CHCl_3$ and diethylether. [3]pseudorotaxane **{[3]CuPR(ClO$_4$)$_4$}** was isolated as greenish solid in yield 79%. Anal. calcd. For **{[3]CuPR(ClO$_4$)$_4$}**, $C_{118}H_{120}Cl_4Cu_2N_{10}O_{32}$ (MW = 2459.16) C, 57.63; H, 4.92; N, 5.70; found: C, 57.39; H, 4.81; N, 5.49. HRMS (ESI-MS) {**[3]CuPR(ClO$_4$)$_4$-2ClO$_4^-$** =$C_{118}H_{120}Cl_2Cu_2N_{10}O_{24}$}$^{2+}$: calcd, *m/z* = 1128.3223; found, *m/z* = 1128.3229; {**[3]CuPR(ClO$_4$)$_4$-3ClO$_4^-$** =$C_{118}H_{120}ClCu_2N_{10}O_{20}$}$^{3+}$: calcd, *m/z* = 719.2320; found, *m/z* = 719.2326. IR (KBr, ν cm$^{-1}$): 378, 391, 673, 721, 1053, 1074, 1118, 1251, 1390, 1454, 1512, 1539, 1577, 1649, 1716, 2854, 2923, 3423, 3442. Absorption spectra studies: $\lambda_{max}$= 282 nm in $CH_3CN$ solvent and molar extinction coefficient value in $CH_3CN$ (ε) = 6.81x10$^4$ M$^{-1}$ cm$^{-1}$.

**Synthesis of [4]pseudorotaxane{[4]CuPR(ClO$_4$)$_6$}:**

**NaphMC** (86.5 mg, 0.15 mmol) in $CHCl_3$ and $Cu(ClO_4)_2.6H_2O$ (55 mg, 0.15 mmol) in $CH_3OH$ were stirred for 2h at RT. After that, the hexadentate chelating ligand (**L3**)(56 mg, 0.05 mmol) was added in situ in the reaction container, resulting [4]pseudorotaxanes *i.e.* penta coordinated Cu(II) templated heteroleptic ternary complex **{[4]CuPR(ClO$_4$)$_6$}**. The reaction was stirred at RT for another 3-4h. Solvent was evaporated and the resultant solid was washed with $CHCl_3$ and diethylether. The green colored solid was isolated as **{[4]CuPR(ClO$_4$)$_6$}** in 71% yield. Anal. calcd. For **[4]CuPR(ClO$_4$)$_6$**, $C_{174}H_{177}Cl_6Cu_3N_{15}O_{48}$ (MW= 3649.69) C, 57.26; H, 4.89; N, 5.76; found: C, 57.01; H, 4.76; N, 5.62. HRMS (ESI-MS) {**[4]CuPR(ClO$_4$)$_6$-2ClO$_4^-$** =$C_{174}H_{177}Cl_4Cu_3N_{15}O_{40}$}$^{2+}$: calcd, *m/z* = 1722.4460; found, *m/z* = 1722.4463, {**[4]CuPR(ClO$_4$)$_6$-3ClO$_4^-$** =$C_{174}H_{177}Cl_3Cu_3N_{15}O_{36}$}$^{3+}$: calcd, *m/z*= 1115.3144; found, *m/z* = 1115.3148. IR (KBr, ν cm$^{-1}$): 379,624, 673, 725, 746, 763, 817, 935, 1093, 1118, 1251, 1278, 1396, 1452, 1504, 1583, 1625, 1724, 2925, 3249, 3423. Absorption spectra studies: $\lambda_{max}$= 283 nm in $CH_3CN$ solvent and molar extinction coefficient value in $CH_3CN$ (ε) = 7.95x10$^4$ M$^{-1}$ cm$^{-1}$.

**Synthesis of Ni(II) templated [n]Pseudorotaxanes (n=2,3,4):**

Ni(II) templated [n]Pseudorotaxanes(n=2,3,4) were prepared by following the similar synthetic procedures as in cases of Cu(II) templated [n]Pseudorotaxanes (n=2,3,4).

**Characterization of {[2]NiPR(ClO$_4$)$_2$}:** yield 71%. Anal. calcd. For **[2]NiPR(ClO$_4$)$_2$**, $C_{49}H_{49}Cl_2NiN_5O_{12}$ (MW = 1029.53) C, 57.16; H, 4.80; N, 6.80; found: C, 56.98; H, 4.71; N, 6.55. HRMS (ESI-MS) {**[2]NiPR(ClO$_4$)$_2$-ClO$_4^-$** =$C_{49}H_{49}ClNiN_5O_8$}$^+$: calcd, *m/z* = 928.2623; found, *m/z* = 928.2621; {**[2]NiPR(ClO$_4$)$_2$-2ClO$_4^-$** =$C_{49}H_{49}NiN_5O_4$}$^{2+}$: calcd, *m/z* = 414.6569; found, *m/z* = 414.6562; Absorption maxima ($\lambda_{max}$) = 274 nm in $CH_3CN$.

**Characterization of {[3]NiPR(ClO$_4$)$_4$}:** yield 64%. Anal. calcd. For {**[3]NiPR(ClO$_4$)$_4$**}, $C_{118}H_{120}Cl_4Ni_2N_{10}O_{32}$ (MW = 2449.46) C, 57.86; H, 4.94; N, 5.72; found: C, 57.42; H, 4.82; N, 5.52. HRMS (ESI-MS) {**[3]NiPR(ClO$_4$)$_4$-ClO$_4^-$** = $C_{118}H_{120}Cl_3Ni_2N_{10}O_{28}$}$^+$: calcd, *m/z* = 2345.6046; found, *m/z* = 2345.6048; {**[3]NiPR(ClO$_4$)$_4$-2ClO$_4^-$** =$C_{118}H_{120}Cl_2Ni_2N_{10}O_{24}$}$^{2+}$: calcd, *m/z* = 1123.3280; found, *m/z* = 1123.3282. Absorption maxima ($\lambda_{max}$) = 283 nm in $CH_3CN$.

**Characterization of {[4]NiPR(ClO$_4$)$_6$}:** yield 49%. Anal. calcd. For {**[4]NiPR(ClO$_4$)$_6$**}, $C_{174}H_{177}Cl_6Ni_3N_{15}O_{48}$ (MW= 3635.13) C, 57.49; H, 4.91; N, 5.78; found: C, 57.23; H, 4.79; N, 5.58. HRMS (ESI-MS) {**[4]NiPR(ClO$_4$)$_6$-2ClO$_4^-$** =$C_{174}H_{177}Cl_4Ni_3N_{15}O_{40}$}$^{2+}$: calcd, *m/z* = 1714.9546; found, *m/z* = 1714.9547. Absorption maxima ($\lambda_{max}$) = 284 nm in $CH_3CN$.

## Conflicts of interest

There are no conflicts to declare.

## Acknowledgements

P.G. gratefully thanks the Science and Engineering Research Board (SERB), New Delhi (Project SR/S1/IC-39/2012) for financial support. S. Bej acknowledges the Council of Scientific & Industrial Research (CSIR), New Delhi for SRF. M. Nandi and T. K. Ghosh acknowledge DST-Inspire and IACS, Kolkata for SRF and post-doctoral fellowship respectively. The authors are thankful to Dr. S. Santra for his valuable suggestion during the work. The single crystal X-ray analysis was performed at the DST-funded National Single Crystal X-ray facility at the School of Chemical Science, IACS.

## References

1. (a)K. Zhu, G. Baggi and S. J. Loeb, *Nat. Chem.*, 2018, **10**, 625-630; (b)V. Balzani, A. Credi and M. Venturi, *Chem. Soc. Rev.*, 2009, **38**, 1542-1550; (c)G. De Bo, M. A. Y. Gall, M. O. Kitching, S. Kuschel, D. A. Leigh, D. J. Tetlow and J. W. Ward, *J. Am. Chem. Soc.*, 2017, **139**, 10875-10879; (d)K.-S. Jeong, K.-J. Chang and Y.-J. An, *Chem. Commun.*, 2003, 1450-1451; (e)J. F. Stoddart, *Angew. Chem., Int. Ed.*, 2017, **56**, 11094-11125; (f)J.-P. Sauvage, *Angew. Chem., Int. Ed.*, 2017, **56**, 11080-11093; (g)W. Yang, Y. Li, H. Liu, L. Chi and Y. Li, *Small*, 2012, **8**, 504-516; (h)J.-P. Collin, C. Dietrich-Buchecker, P. Gavina, M. C. Jimenez-Molero and J.-P. Sauvage, *Acc. Chem. Res.*, 2001, **34**, 477-487; (i)J. C. Olsen, A. C. Fahrenbach, A. Trabolsi, D. C. Friedman, S. K. Dey, C. M. Gothard, A. K. Shveyd, T. B. Gasa, J. M. Spruell, M. A. Olson, C. Wang, H. P. Jacquot de Rouville, Y. Y. Botros and J. F. Stoddart, *Org.*

*Biomol. Chem.*, 2011, **9**, 7126-7133; (j)S. Goldup, *Nature*, 2018, **557**, 39-40.
2. (a)C. A. Schalley, K. Beizai and F. Voegtle, *Acc. Chem. Res.*, 2001, **34**, 465-476; (b)A. K. Mandal, M. Gangopadhyay and A. Das, *Chem. Soc. Rev.*, 2015, **44**, 663-676.
3. (a)Y. Jiang, J.-B. Guo and C.-F. Chen, *Chem. Commun.*, 2010, **46**, 5536-5538; (b)X. Ma, R. Sun, W. Li and H. Tian, *Polym. Chem.*, 2011, **2**, 1068-1070.
4. M. J. Langton and P. D. Beer, *Acc. Chem. Res.*, 2014, **47**, 1935-1949.
5. (a)N. G. White and P. D. Beer, *Org. Biomol. Chem.*, 2013, **11**, 1326-1333; (b)J. Y. C. Lim, I. Marques, V. Felix and P. D. Beer, *Angew. Chem., Int. Ed.*, 2018, **57**, 584-588.
6. (a)J.-J. Lee, A. G. White, J. M. Baumes and B. D. Smith, *Chem. Commun.*, 2010, **46**, 1068-1069; (b)J. M. Baumes, J. J. Gassensmith, J. Giblin, J.-J. Lee, A. G. White, W. J. Culligan, W. M. Leevy, M. Kuno and B. D. Smith, *Nat. Chem.*, 2010, **2**, 1025-1030.
7. (a)J. D. Crowley, S. M. Goldup, N. D. Gowans, D. A. Leigh, V. E. Ronaldson and A. M. Z. Slawin, *J. Am. Chem. Soc.*, 2010, **132**, 6243-6248; (b)C. Browne, T. K. Ronson and J. R. Nitschke, *Angew. Chem., Int. Ed.*, 2014, **53**, 10701-10705; (c)A. Inthasot, S.-T. Tung and S.-H. Chiu, *Acc. Chem. Res.*, 2018, **51**, 1324-1337; (d)E. A. Neal and S. M. Goldup, *Chem. Sci.*, 2015, **6**, 2398-2404; (e)J. E. Beves, B. A. Blight, C. J. Campbell, D. A. Leigh and R. T. McBurney, *Angew. Chem., Int. Ed.*, 2011, **50**, 9260-9327; (f)S. W. Robinson, C. L. Mustoe, N. G. White, A. Brown, A. L. Thompson, P. Kennepohl and P. D. Beer, *J. Am. Chem. Soc.*, 2015, **137**, 499-507; (g)M. Cirulli, A. Kaur, J. E. M. Lewis, Z. Zhang, J. A. Kitchen, S. M. Goldup and M. M. Roessler, *J. Am. Chem. Soc.*, 2019, **141**, 879-889; (h)S. Prusty, S. Krishnaswamy, S. Bandi, B. Chandrika, J. Luo, J. S. McIndoe, G. S. Hanan and D. K. Chand, *Chem. - Eur. J.,* 2015, **21**, 15174-15187.
8. (a)Y. Wang, T. Cheng, J. Sun, Z. Liu, M. Frasconi, W. A. Goddard and J. F. Stoddart, *J. Am. Chem. Soc.*, 2018, **140**, 13827-13834; (b)M. Bruschini, G. Ercolani, S. Gallina and P. Mencarelli, *J. Org. Chem.*, 2018, **83**, 11446-11449; (c)D.-H. Qu and H. Tian, *Chem. Sci.*, 2011, **2**, 1011-1015.
9. E. V. Dzyuba, L. Kaufmann, N. L. Low, A. K. Meyer, H. D. F. Winkler, K. Rissanen and C. A. Schalley, *Org. Lett.*, 2011, **13**, 4838-4841.
10. (a)M. J. Langton, I. Marques, S. W. Robinson, V. Felix and P. D. Beer, *Chem. - Eur. J.*, 2016, **22**, 185-192; (b)N. L. Kilah, M. D. Wise, C. J. Serpell, A. L. Thompson, N. G. White, K. E. Christensen and P. D. Beer, *J. Am. Chem. Soc.*, 2010, **132**, 11893-11895.
11. (a)T. Legigan, B. Riss-Yaw, C. Clavel and F. Coutrot, *Chem. - Eur. J.*, 2016, **22**, 8835-8847; (b)J.-P. Collin and J.-P. Sauvage, *Chem. Lett.*, 2005, **34**, 742-747; (c)T. Kraus, M. Budesinksy, J. Cvacka and J.-P. Sauvage, *Angew. Chem., Int. Ed.*, 2006, **45**, 258-261.
12. (a)C. Gozalvez, J. L. Zafra, A. Saeki, M. Melle-Franco, J. Casado and A. Mateo-Alonso, *Chem. Sci.*, 2019, **10**, 2743–2749; (b)D. R. Kohn, L. D. Movsisyan, A. L. Thompson and H. L. Anderson, *Org. Lett.*, 2017, **19**, 348-351.
13. (a)B. H. Northrop, S. J. Khan and J. F. Stoddart, *Org. Lett.*, 2006, **8**, 2159-2162; (b)K. Zhu, V. N. Vukotic and S. J. Loeb, *Chem. - Asian J.*, 2016, **11**, 3258-3266; (c)A. K. Mandal, M. Suresh and A. Das, *Org. Biomol. Chem.*, 2011, **9**, 4811-4817; (d)Z. Niu, C. Slebodnick and H. W. Gibson, *Org. Lett.*, 2011, **13**, 4616-4619; (e)F. Huang, F. R. Fronczek and H. W. Gibson, *J. Am. Chem. Soc.*, 2003, **125**, 9272-9273; (f)K. Ghosh, H.-B. Yang, B. H. Northrop, M. M. Lyndon, Y.-R. Zheng, D. C. Muddiman and P. J. Stang, *J. Am. Chem. Soc.*, 2008, **130**, 5320-5334; (g)W. Jiang, H. D. F. Winkler and C. A. Schalley, *J. Am. Chem. Soc.*, 2008, **130**, 13852-13853; (h)C. R. Benson, A. I. Share, M. G. Marzo and A. H. Flood, *Inorg. Chem.*, 2016, **55**, 3767-3776; (i)X. Yan, X. Chi, P. Wei, M. Zhang and F. Huang, *Eur. J. Org. Chem.*, 2012, **2012**, 6351-6356; (j)L. Gao, C. Han, B. Zheng, S. Dong and F. Huang, *Chem. Commun.*, 2013, **49**, 472-474; (k)T.-G. Zhan, L. Wu, Z. Zhao, Z.-B. Zhou, M.-Y. Yun, J. Wei, S.-T. Zheng, H.-H. Yin and K.-D. Zhang, *Chem. Commun.*, 2017, **53**, 5396-5399; (l)Z.-J. Zhang, H.-Y. Zhang, L. Chen and Y. Liu, *J. Org. Chem.*, 2011, **76**, 8270-8276; (m)S. Saha, I. Ravikumar and P. Ghosh, *Chem. - Eur. J.*, 2011, **17**, 13712-13719; (n)J.-P. Collin, J.-P. Sauvage, Y. Trolez and K. Rissanen, *New J. Chem.*, 2009, **33**, 2148-2154; (o)S. Saha, I. Ravikumar and P. Ghosh, *Chem. Commun.*, 2011, **47**, 6272-6274.
14. (a)S. Saha and J. F. Stoddart, *Chem. Soc. Rev.*, 2007, **36**, 77-92; (b)L. Yuan, R. Wang and D. H. Macartney, *J. Org. Chem.*, 2007, **72**, 4539-4542; (c)H. Xing, H. Wang, X. Yan and X. Ji, *Dalton Trans.*, 2015, **44**, 11264-11268; (d)F. Huang, I. A. Guzei, J. W. Jones and H. W. Gibson, *Chem. Commun.*, 2005, 1693-1695; (e)S. Santra, S. Bej, M. Nandi, P. Mondal and P. Ghosh, *Dalton Trans.*, 2017, **46**, 13300-13313; (f)S. Santra, S. Mukherjee, S. Bej, S. Saha and P. Ghosh, *Dalton Trans.*, 2015, **44**, 15198-15211; (g)M. Nandi, S. Santra, B. Akhuli and P. Ghosh, *Dalton Trans.*, 2017, **46**, 7421-7433; (h)M. Gangopadhyay, A. K. Mandal, A. Maity, S. Ravindranathan, P. R. Rajamohanan and A. Das, *J. Org. Chem.*, 2016, **81**, 512-521; (i)Q.-W. Zhang, J. Zajicek and B. D. Smith, *Org. Lett.*, 2018, **20**, 2096-2099; (j)K. M. Mullen, K. D. Johnstone, D. Nath, N. Bampos, J. K. M. Sanders and M. J. Gunter, *Org. Biomol. Chem.*, 2009, **7**, 293-303; (k)W. Jiang, D. Sattler, K. Rissanen and C. A. Schalley, *Org. Lett.*, 2011, **13**, 4502-4505.
15. (a)J. Voignier, J. Frey, T. Kraus, M. Budesinsky, J. Cvacka, V. Heitz and J.-P. Sauvage, *Chem. - Eur. J.*, 2011, **17**, 5404-5414; (b)J. J. Danon, D. A. Leigh, P. R. McGonigal, J. W. Ward and J. Wu, *J. Am. Chem. Soc.*, 2016, **138**, 12643-12647; (c)J. E. M. Lewis, P. D. Beer, S. J. Loeb and S. M. Goldup, *Chem. Soc. Rev.*, 2017, **46**, 2577-2591.
16. S. Bej and P. Ghosh, *Dalton Trans.*, 2018, **47**, 13408-13418.
17. K. Hara, H. Sugihara, L. P. Singh, A. Islam, R. Katoh, M. Yanagida, K. Sayama, S. Murata and H. Arakawa, *J. Photochem. Photobiol., A*, 2001, **145**, 117-122.

Journal Name ARTICLE

## Table of Contents

View Article Online
DOI: 10.1039/C9DT01067J

# Cu(II) templated formation of [n]Pseudorotaxanes (n= 2,3,4) using a tris-amino ether macrocyclic wheel and multidentate axles

Somnath Bej, Mandira Nandi, Tamal Kanti Ghosh and Pradyut Ghosh*

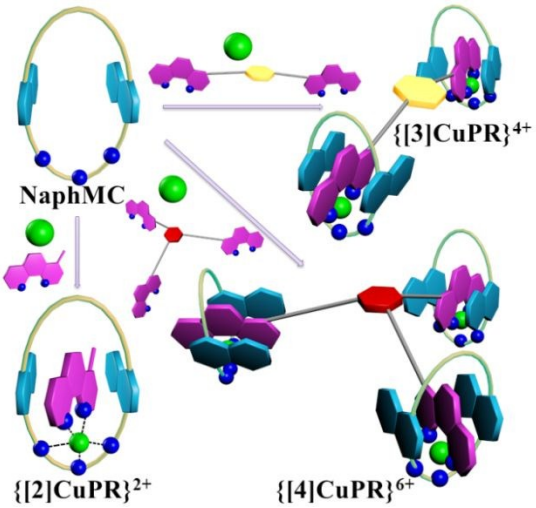


Systematic development of mono-, bi- and tri-nuclear [n]Pseudorotaxanes (n=2,3,4) via Cu(II) templation and π–π stacking interactions.